Al-Hadidi MS, Goss JP, Briddon PR, Al-Hamadany RA, Ahmed ME, Rayson MJ. **Density functional simulation of carbon at the titanium site in perovskite barium titanate**. ***In: 12TH EUROPHYSICAL 12th Europhysical Conference on Defects in Insulating Materials (EURODIM 2014)*. 2015, Canterbury, UK: IOP Publishing.**

Density functional simulation of carbon at the titanium site in perovskite barium titanate

2015 IOP Conf. Ser.: Mater. Sci. Eng. 80 012002

(http://iopscience.iop.org/1757-899X/80/1/012002)

IOP Conf. Series: Materials Science and Engineering **80** (2015) 012002 doi:10.1088/1757-899X/80/1/012002

Density functional simulation of carbon at the titanium site in perovskite barium titanate

Meaad S AL-Hadidi[1,2], J P Goss[1], P R Briddon[1], Raied A Al-Hamadany[1,3], Mariam E Ahmed[4] and M J Rayson[5]

[1]Electrical and Electronic Engineering, Newcastle University, Newcastle upon Tyne, UK
[2]Renewable Energy Department, Science College, Mosul University, Mosul, Iraq
[3]Physics Department, Science College, Thi-Qar University, Nasiriyah, Iraq
[4]Physics Department, Tripoli University, Tripoli, Libya
[5]Department of Chemistry, University of Surrey, Guildford, Surrey GU2 7XH, United Kingdom

E-mail: m.al-hadidi@ncl.ac.uk

Abstract. The perovskite family includes many titanates which have been used in various applications. $BaTiO_3$ is interesting due to its room-temperature ferroelectric properties and relative low toxicity. Organic precursors present during growth make carbon a potentially key impurity, which would subsequently impact upon the $BaTiO_3$ properties. This paper presents a density function study of the structural and electronic properties of carbon substituting for Ti in rhombohedral $BaTiO_3$. The local vibrational modes of the defect centre has been calculated and suggested as a possible route to experimental identification.

1. Introduction

$BaTiO_3$ is a ferroelectric material with a high dielectric constant and low loss characteristics, widely utilised in the manufacture of electronic components such as multilayer dielectric capacitors and high refractive index thin films[1]. Its piezoelectric and pyroelectric properties lend it to passive infrared detectors[2], piezoelectric actuators and sonar devices[3], and its positive temperature coefficient of resistivity allows it to be used in sensor applications[3].

In recent years, significant amount of experimental and theoretical study has been directed at ferroelectric perovskite $BaTiO_3$[4, 5, 6, 7, 8, 9, 10, 11, 12, 13, 14]. Both theoretical and experimental studies have shown that intrinsic and extrinsic defects affect the electronic structure, photonic properties, remnant polarisation, motion of domain walls, dielectric constant and leakage current in this material[15, 16, 17, 18]. For example, pentavalent dopants (Sb, Nb and Ta) can produce semiconductor by substitution at Ti^{+4} sites[1], and oxygen vacancies also act electrically[19]. Indeed, addition of impurities to $BaTiO_3$ is needed to achieve the desired enhancement of, for example, photoconductivity, piezoelectricity and positive temperature coefficient of resistivity[20, 3, 21].

Given the dependence of the $BaTiO_3$ properties upon both stoichiometry and purity, the crystal growth techniques used are highly significant. Various different techniques have been used to synthesis thin films, including solid-state reaction[22], the sol-gel method[23, 24, 25, 16, 19], mechanochemical synthesis[26, 27], solvothermal synthesis methods[28], sputter deposition[29], pulsed-laser deposition[30], chemical vapour deposition[31] and atomic layer deposition[31, 32],

in order to eliminate problems such as heterogeneity, impurities, inaccurate thickness control and the poor electrical properties of sintered ceramics. In several of these methods organic precursors are used for Ba sources, and subsequent carbon contamination has been reported in $BaTiO_3$ thin films[33, 25, 26, 32]. For example, sharp peaks at 1425, 1050, 860, and 695 cm^{-1} were observed and attributed to the carbonate ions (CO_3^{-2})[34].

In this paper, we present the results of first principles calculations on the geometry, electronic structure, vibrational modes and reorientation barrier of carbon substituting for Ti in $BaTiO_3$.

2. Computational details

The properties of carbon substituting for Ti in rhombohedral $BaTiO_3$ are calculated using first-principles density functional theory within the local density approximation[35]. The self-consistence total energy calculations were performed using the AIMPRO computer code[36, 37] based on the stable and efficient preconditioned conjugate gradients method with the optimised structures having forces of $< 10^{-3}$ atomic units and the final structural optimisation step is required to result in a reduction in the total energy of less than 10^{-5} Ha.

Atoms are modelled using norm-conserving, separable pseudo potentials[38] (valance sets of Ba, Ti, O and C are $5s^25p^66s^2$, $3s^23p^63d^24s^2$, $2s^22p^4$ and $2s^22p^2$, respectively), with the Kohn-Sham eigen-functions expanded using atom centred Gaussian basis sets[39], comprised from four independent sets of s, p and d type functions. Matrix elements of the Hamiltonian are determined using a plane-wave expansion of the density and Kohn-Sham potential[40] with a cut-off of 150 Ha, resulting in absolute convergence of the total energy with respect to the expansion of the charge density to better than 0.03 meV.

For bulk rhombohedral $BaTiO_3$ symmetry, our computational approach yields an equilibrium lattice parameters of 3.97 Å and 89.85°, within 1% of experiment[41, 42]. The calculated bandgap is 2.3 eV, reflecting the well documented underestimate arising from the underpinning methodology. Our estimate is consistent with previous comparable calculations[43].

To model defects, we use the same type of cell detailed previously[44], consisting of 160 host atoms. The Brillouin zone is sampled using a uniform $2 \times 2 \times 2$ Monkhorst-Pack mesh[45].

Vibrational modes have been calculated by obtaining the second derivatives of the energy with respect to atomic positions, which are then assembled into the dynamical matrix. The derivatives are determined using a finite-difference approximation based upon analytical forces obtained with atomic displacement of 0.2 atomic units.

Finally, reaction pathways and activation energies are determined using the climbing nudged-elastic-band (NEB) method[46, 47], and the convergence of the saddle point energy with respect to the number of images and the image-forces has been established to within a few meV.

3. Results and discussion

3.1. Defect geometry

We start with the geometry of carbon substitution of titanium, C_{Ti}, which may be anticipated on the grounds of both C and Ti being group-IV elements[48]. The first structure analysed was created from the octahedral symmetry, with a Ti ion simply replaced with carbon. In the absence of any symmetry constraint, the optimised structure of C_{Ti} exhibits significant structural change from the initial geometry. The carbon is displaced from the centre where it was initially co-ordinated with six oxygen ions, toward the centre of a triangular group composed of three oxygen ions, as shown in figure 1(b). The final structure has three C–O bonds 35% shorter than the host Ti–O distances. The equilibrium geometry can be clearly identified as a carbonate group ion. To further support this view it is noted that the calculated C-O bond-lengths of 1.29 Å are close to those of the carbonate group[49, 50] and those in witherite[51].

We now turn to the impact that the formation of the carbonate group has upon the electronic properties of the material.

3.2. Electronic structure

The band structure for C_{Ti} is shown in figure 1(c). The inclusion of a carbon atom at a Ti site does not have any significant effect on the band-gap, which we note is in contrast to the situation with C_{Ti} in cubic $SrTiO_3$[48]. Carbon substitution for titanium in $BaTiO_3$ is therefore expected to lead to electrically inactive defects, i.e. these centres are not expected to introduce any states in the band-gap that would lead to a change of charge state.

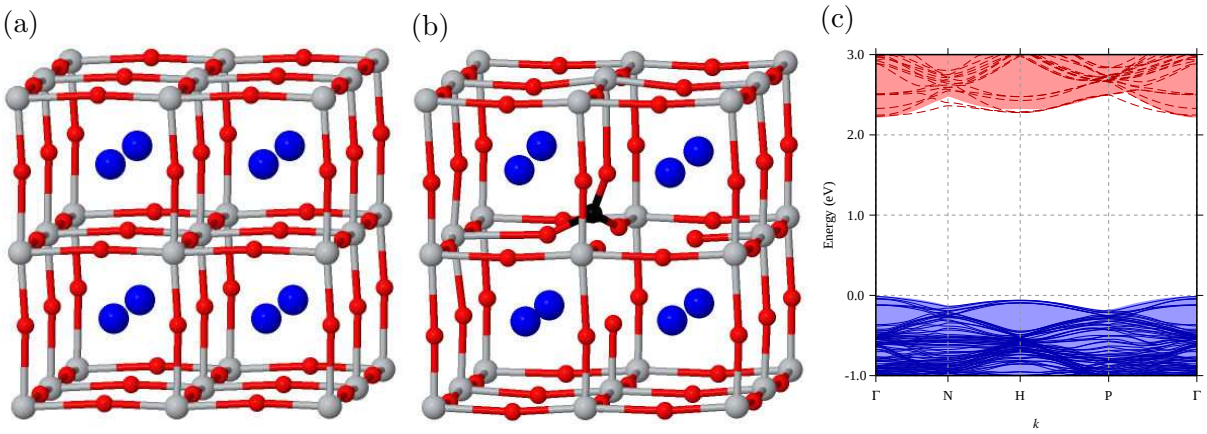

Figure 1. Schematics of (a) pure $BaTiO_3$, and (b) C_{Ti} in $BaTiO_3$. Blue, grey, red and black atoms represent Ba, Ti, O and C respectively. Vertical and horizontal axes are approximately [001] and [010], respectively, with the tilted view adopted to aid clarity. (c) shows the band structure of C_{Ti} in $BaTiO_3$ in the first Brillouin zone of the supercell, plotted along high-symmetry branches. Labelling on the x-axis follows the conventions for special points at the zone-boundary for the bcc Brillouin zone. Occupied and empty bands are shown in solid blue and dashed red lines, respectively. The underlying shaded areas show the regions of the bands for the corresponding C-free supercell. The zero on the energy scale is defined to be the highest occupied state in each case.

3.3. Vibrational modes

Turning to vibrational characteristics, we find that the calculated frequencies are consistent with C_{Ti} resulting in the formation of carbonate ions. A set of characteristic local vibrational modes lies above the one-phonon maximum, which could prove highly effective in the experimental identification of this centre: with a nearly degenerate C–O stretch mode at $1383\,cm^{-1}$ and $1379\,cm^{-1}$, and a breathing stretch-mode is at $1061\,cm^{-1}$. These are close to the experimental values of CO_3^{-2} gas phase[52] which have E' and A_1' stretch modes lying around $1415\,cm^{-1}$ and 1064cm, respectively, and also agree both with the modes detected in $BaTiO_3$[34], and with those modes assigned to the carbonate groups in $BaCO_3$[53]. Lower frequency modes of the carbonate group are also present for C_{Ti}, but are resonant with the one-phonon density of states. All three local modes listed here are, by symmetry, infra-red and Raman active, and given sufficient concentrations one might seek to confirm the presence of this form of carbon centre directly via either IR or Raman spectroscopy.

3.4. Carbonate group reorientation

Finally, the energetics for carbonate group reorientation have been predicted. The initial and final structures are shown in figure 2(a) and (b), and the energy profile along the minimum energy path between them in figure 2(c). The energy difference between initial and final structure

has been calculated to be about 50 meV, which is related to non-equivalent in the defect with respect to the rhombohedral distortion. The activation energy for reorientation process has been calculated to be around 2.5 eV. The barrier is found to be high in energy compared to, for example, diffusion of the oxygen vacancy, since the reorientation requires the breaking and formation of strong covalent C–O bonds. It is noted, however, that this activation energy is similar to the equivalent path in cubic $SrTiO_3$[48]. The high barrier is expected to lead to slow reorientation at room temperature, which will impact upon the hysteresis seen in the material under an applied electric field.

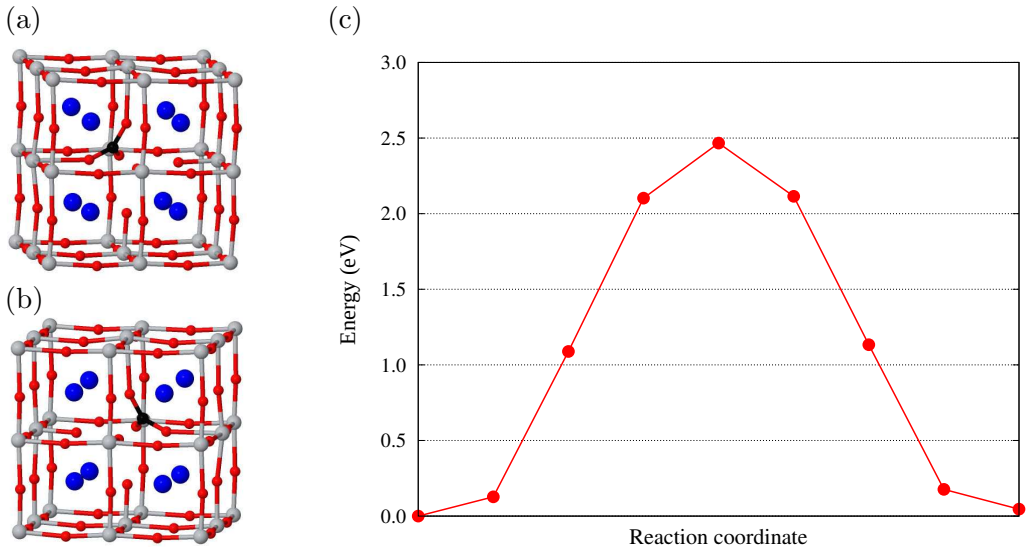

Figure 2. Schematic of (a) initial, and (b) final structure of C_{Ti} in $BaTiO_3$ in a simple reorientation process. Colours and orientation are as indicated in figure 1. (c) Calculated reorientation barrier of C_{Ti} in $BaTiO_3$ between initial and final structure, with circles showing the energies of the 9 images in the NEB algorithm.

4. Summary and conclusions

In summary, based on first-principles density-functional calculations, the characteristics of carbon impurities substituting for titanium in rhombohedral $BaTiO_3$ have been examined, including the structural configuration, electronic properties, vibrational modes and reorientation barrier. The calculations reveal that carbon energetically favours the formation of carbonate groups and suggest that the carbon substituting of titanium is electrically passive, so that C_{Ti} is predicted to have a minimal impact upon the electrical conductivity of $BaTiO_3$. The vibrational frequencies associated with defect centre have been determined and compared with available theoretical and experiment values. These spectroscopic properties are a clear route to experimental identification of this defect. Finally, the reorientation barrier for the carbonate group for C_{Ti} has been estimated, and because the process involves the breaking and forming of C–O covalent bonds, the barrier has a relatively high value which will in general impact upon ferroelectric hysteresis.

References

[1] Chatterjee S, Stojanovic BD and Maiti H, 2003 *Mater. Chem. Phys.* **78** 702
[2] Akcay G, Zhong S, Alpay S and Mantese J, 2006 *Solid State Commun.* **137** 589
[3] Ertug B, 2013 *American Journal of Engineering Research* **2** 1
[4] Ishidate T, Abe S, Takahashi H and Môri N, 1997 *Phys. Rev. Lett.* **78** 2397

[5] Piskunov S, Heifets E, Eglitis R and Borstel G, 2004 *Comp. Mater. Sci.* **29** 165–178
[6] Stuhrmann HB, 1970 *Acta Crystallogr. A* **26** 297
[7] Kinoshita K and Yamaji A, 1976 *J. Appl. Phys.* **47** 371
[8] Frey MH and Payne DA, 1996 *Phys. Rev. B* **54** 3158
[9] King-Smith RD and Vanderbilt D, 1994 *Phys. Rev. B* **49** 5828
[10] Saha S, Sinha TP and Mookerjee A, 2000 *Phys. Rev. B* **62** 8828
[11] Roussev R and Millis AJ, 2003 *Phys. Rev. B* **67** 014105
[12] Zhong W, Vanderbilt D and Rabe KM, 1994 *Phys. Rev. Lett.* **73** 1861
[13] Tanaka T, Matsunaga K, Ikuhara Y and Yamamoto T, 2003 *Phys. Rev. B* **68** 205213
[14] Miura K, Azuma M and Funakubo H, 2011 *Materials* **4** 260
[15] Pöykkö S and Chadi DJ, 1999 *Phys. Rev. Lett.* **83** 1231
[16] Ghosh VJ, Nielsen B and Friessnegg T, 2000 *Phys. Rev. B* **61** 207
[17] Schwartz RN and Wechsler BA, 2000 *Phys. Rev. B* **61** 8141
[18] Stashans A and Chimborazo J, 2002 *Phil. Mag. B* **82** 1145
[19] Yoo HI, Chang MW, Oh TS, Lee CE and Becker KD, 2007 *J. Appl. Phys.* **102** 093701
[20] Chen X, Lu W and Shen SC, 2004 *Solid State Commun.* **130** 641
[21] Rao M, Ramesh KaRM and Rao B, 2013 *Adv. in Mater. Phys. and Chem.* **87** 77
[22] Potdar H, Deshpande S and Date S, 1999 *Mater. Chem. Phys.* **58** 121
[23] Cho W, 1998 *J. Phys. Chem. Solids* **59** 659
[24] Cho W and Hamada E, 1998 *J. Alloys and Compounds* **266** 118
[25] Li B, Wang X and Li L, 2003 *Mater. Chem. Phys.* **78** 292
[26] Stojanovic B, Simoes A, Paiva-Santos C, Jovalekic C, Mitic V and Varela J, 2005 *J. Euro. Ceramic Soc.* **25** 1985
[27] Stojanovic BD, Jovalekic C, Vukotic V, Simoes AZ and Varela JA, 2005 *Ferroelectrics* **319** 65
[28] Lee H, Moon S, Choi C and Kim DK, 2012 *J. Am. Ceramic Soc.* **95** 2429
[29] Reynolds GJ, Kratzer M, Dubs M, Felzer H and Mamazza R, 2012 *Materials* **5** 575
[30] Norton MG, Scarfone C, Li J, Carter CB and Mayer JW, 1991 *J. Mater. Res.* **6** 2022
[31] Holme TP and Prinz FB, 2007 *J. Phys. Chem. A* **111** 8147
[32] Vehkamäki M, Hatanpää T, Ritala M, Leskelä M, Väyrynen S and Rauhala E, 2007 *Chem. Vapor Dep.* **13** 239
[33] Vinothini V, Singh P and Balasubramanian M, 2006 *Ceramics International* **32** 99
[34] Tsay J, Fang T, Gubiotti TA and Ying JY, 1998 *J. Mater. Sci.* **33** 3721–3727
[35] Perdew JP and Wang Y, 1992 *Phys. Rev. B* **45** 13244–13249
[36] Briddon PR and Jones R, 2000 *Phys. Status Solidi B* **217** 131–171
[37] Rayson MJ and Briddon PR, 2008 *Computer Phys. Comm.* **178** 128–134
[38] Hartwigsen C, Goedecker S and Hutter J, 1998 *Phys. Rev. B* **58** 3641–3662
[39] Goss JP, Shaw MJ and Briddon PR, 2007 In *Theory of Defects in Semiconductors*, edited by DA Drabold and SK Estreicher, volume 104 of *Topics in Applied Physics*. Springer, Berlin/Heidelberg, pages 69–94
[40] Rayson MJ and Briddon PR, 2009 *Phys. Rev. B* **80** 205104
[41] Berlincourt D and Jaffe H, 1958 *Phys. Rev.* **111** 143
[42] Hewat AW, 1973 *Ferroelectrics* **6** 215
[43] Ghosez P, Gonze X and Michenaud JP, 1999 *Ferroelectrics* **220** 1
[44] Al-Hamadany R, Goss JP, Briddon PR, Mojarad SA, Al-Hadidi M, ONeill AG and Rayson MJ, 2013 *J. Appl. Phys.* **113** 024108
[45] Monkhorst HJ and Pack JD, 1976 *Phys. Rev. B* **13** 5188–5192
[46] Henkelman G, Uberuaga BP and Jónsson H, 2000 *J. Chem. Phys.* **113** 9901–9904
[47] Henkelman G and Jónsson H, 2000 *J. Chem. Phys.* **113** 9978–9985
[48] Al-Hadidi MS, Goss JP, Briddon PR, Al-Hamadany RA and Ahmed ME, 2013 *J. Phys. Conf. Ser.* **472** 012006
[49] Adler HH and Kerr PF, 1963 *Am. Miner.* **48** 839–853
[50] Gagliardi L and Roos BO, 2002 *Inorg. Chem.* **41** 1315
[51] Antao SM and Hassan I, 2007 *Phys. and Chem. Minerals* **34** 573–580
[52] Tavender SM, Johnson SA, Balsom D, Parker wA and Bisby RH, 1999 *Laser Chem.* **19** 311–316
[53] Krishnamurti D, 1960 *Proceedings of the Indian Academy of Sciences - Section A* **51** 285–295